

# AAVrh10 vector corrects pathology in animal models of GM1 gangliosidosis and achieves widespread distribution in the CNS of nonhuman primates

Michaël Hocquemiller,<sup>1</sup> Laura Giersch,<sup>1</sup> Xin Mei,<sup>1</sup> Amanda L. Gross,<sup>2</sup> Ashley N. Randle,<sup>2</sup> Heather L. Gray-Edwards,<sup>2</sup> Judith A. Hudson,<sup>3</sup> Sophia Todeasa,<sup>5</sup> Lorelei Stoica,<sup>5</sup> Douglas R. Martin,<sup>2,4</sup> Miguel Sena-Esteves,<sup>5</sup> Karen Aiach,<sup>1</sup> and Ralph Laufer<sup>1</sup>

<sup>1</sup>Lysogene, 18–20 rue Jacques Dulud, 92200 Neuilly-sur-Seine, France; <sup>2</sup>Scott-Ritchey Research Center, Auburn University College of Veterinary Medicine, Auburn, AL 36849, USA; <sup>3</sup>Department of Clinical Sciences, Auburn University College of Veterinary Medicine, Auburn, AL 36849, USA; <sup>4</sup>Department of Anatomy, Physiology, and Pharmacology, Auburn University College of Veterinary Medicine, Auburn, AL 36849, USA; <sup>5</sup>Department of Neurology, Horae Gene Therapy Center, University of Massachusetts Medical School, Worcester, MA 01605, USA

**GM1 gangliosidosis is a rare, inherited neurodegenerative disorder caused by mutations in the GLB1 gene, which encodes the lysosomal hydrolase acid  $\beta$ -galactosidase ( $\beta$ -gal).  $\beta$ -gal deficiency leads to toxic accumulation of GM1 ganglioside, predominantly in the central nervous system (CNS), resulting in progressive neurodegeneration. LYS-GM101 is an AAVrh.10-based gene therapy vector carrying the human GLB1 cDNA. The efficacy of intra-cerebrospinal fluid injection of LYS-GM101 analogs was demonstrated in GM1 mouse and cat models with widespread diffusion of  $\beta$ -gal and correction of GM1 ganglioside accumulation in the CNS without observable adverse effects. Clinical dose selection was performed, based on a good-laboratory-practice study, in nonhuman primates (NHPs) using the clinical LYS-GM101 vector. A broadly distributed increase of  $\beta$ -gal activity was observed in NHP brain 3 months after intra-cisterna magna injection of LYS-GM101 at  $1.0 \times 10^{12}$  vg/mL CSF and  $4.0 \times 10^{12}$  vg/mL CSF, with 20% and 60% increases compared with vehicle-treated animals, respectively. Histopathologic examination revealed asymptomatic adverse changes in the sensory pathways of the spinal cord and dorsal root ganglia in both sexes and at both doses. Taken as a whole, these pre-clinical data support the initiation of a clinical study with LYS-GM101 for the treatment of GM1 gangliosidosis.**

## INTRODUCTION

GM1 gangliosidosis (OMIM: 230500) is an autosomal recessive neurodegenerative disorder caused by mutations in the galactosidase beta 1 (GLB1) gene leading to deficiency of the lysosomal hydrolase acid  $\beta$ -galactosidase ( $\beta$ -gal; EC 3.2.1.23).<sup>1</sup> Reduced or absent activity of  $\beta$ -gal is associated with lysosomal accumulation of GM1 ganglioside in different tissues and particularly in the central nervous system (CNS). Clinical features are predominantly those of a neurodegenerative disorder but also include hepatosplenomegaly, coarse facial features, and skeletal dysostosis. Neurological features span a contin-

uum, with decreasing residual  $\beta$ -gal activity leading to increasing clinical severity and earlier onset of disease.<sup>2</sup> Four clinically distinct phenotypes have been described, based on the age at which symptoms appear: infantile, late infantile, juvenile, and adult onset.<sup>3</sup> The incidence of GM1 gangliosidosis is estimated at 1 in 100,000–200,000 live births, but it is higher in certain ethnic groups and countries.<sup>1</sup> Currently there is no treatment for GM1 gangliosidosis.

Pre-clinical studies using murine and feline models of GM1 gangliosidosis have demonstrated that adeno-associated viral (AAV) vectors can be used to deliver the normal GLB1 cDNA and restore  $\beta$ -gal activity in the brain and spinal cord via several routes of administration: intraparenchymal,<sup>4–7</sup> intra-cerebrospinal fluid (CSF),<sup>8,9</sup> or intravenously.<sup>10,11</sup> Restoration of  $\beta$ -gal activity in the CNS led to partial or complete reversion of disease phenotypes in these animal models, even with restoration of only ~20% of normal activity levels.<sup>11</sup> Ongoing clinical studies to treat GM1 gangliosidosis by gene therapy use AAV9 for intravenous delivery (ClinicalTrials.gov identifier NCT03952637) and AAVrh10 or AAVhu68 for CSF-mediated delivery via the cisterna magna (NCT04273269 or NCT04713475, respectively).

The aim of the present study was to evaluate the impact of AAVrh.10 vector carrying species-specific GLB1 on enzyme activity and lysosomal storage in the CNS of mouse and feline disease models of GM1 gangliosidosis. Different routes of CNS delivery were investigated, including intraparenchymal and intracerebroventricular

Received 12 July 2022; accepted 5 October 2022;  
<https://doi.org/10.1016/j.omtm.2022.10.004>.

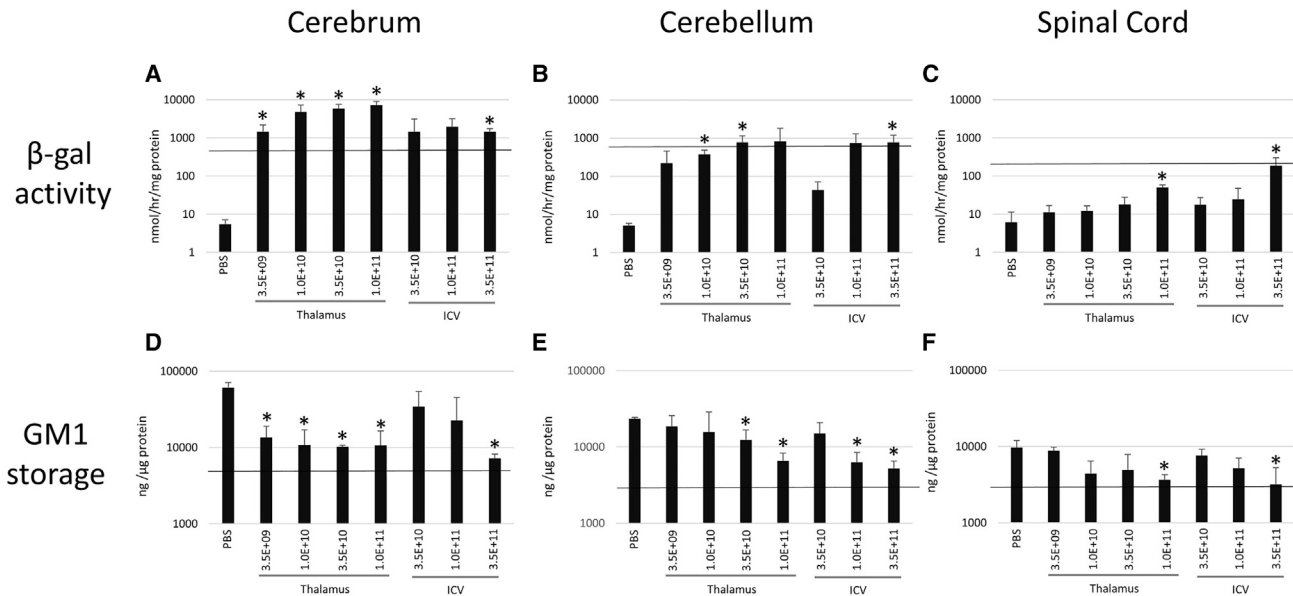
**Correspondence:** Michaël Hocquemiller, Lysogene, 18–20 rue Jacques Dulud, 92200 Neuilly-sur-Seine, France.

**E-mail:** [michael.hocquemiller@lysogene.com](mailto:michael.hocquemiller@lysogene.com)

**Correspondence:** Ralph Laufer, Lysogene, 18–20 rue Jacques Dulud, 92200 Neuilly-sur-Seine, France.

**E-mail:** [ralph.laufer@lysogene.com](mailto:ralph.laufer@lysogene.com)





**Figure 1.  $\beta$ -gal enzyme activity and GM1 ganglioside levels in the mouse CNS at 1 month**

AAVrh.10-m $\beta$ gal was injected bilaterally in thalamus ( $2 \times 2.22 \mu\text{L}/\text{thalamus}$ ) or cerebral lateral ventricle ( $14.8 \mu\text{L}$ ). Mice ( $n = 4-6$ ) per group were euthanized at 1 month post injection and  $\beta$ -gal activity (A–C) and GM1 ganglioside storage (D–F) measured in cerebrum (A and D), cerebellum (B and E), and spinal cord (C and F). \* $p < 0.05$  compared with PBS (GM1 gangliosidosis animals injected with PBS via thalamus and i.c.v. combined). Black line corresponds to normal levels assessed from non-injected wild-type mice.

(i.c.v.) in GM1 gangliosidosis mice and i.c.v., intra-cisterna magna (i.c.m.), and intrathecal lumbar (i.t.l.) in the GM1 gangliosidosis cat model. In addition, we investigated in a good-laboratory-practice (GLP) study whether the clinical vector (LYS-GM101) carrying human GLB1, administered into the cisterna magna of nonhuman primates (NHPs), was able to safely achieve therapeutically relevant  $\beta$ -gal expression and broad enzyme distribution in a brain with an architecture and size more close to human, to confirm the scalability of this approach.

## RESULTS



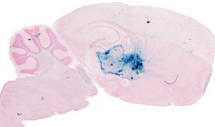
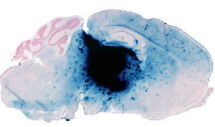

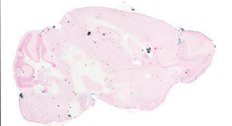
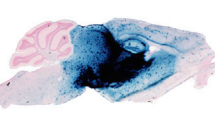
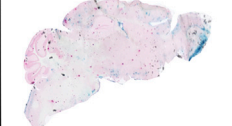
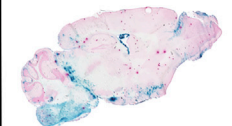
### Mouse study

The efficacy of AAVrh.10-m $\beta$ gal (murine analog of LYS-GM101) in restoring  $\beta$ -gal levels and reducing GM1 ganglioside levels in the CNS was evaluated in a dose-response study using GLB1 knockout mice, a well-established model of GM1 gangliosides,<sup>12</sup> which replicates several clinical and biochemical features of infantile GM1 gangliosidosis, with low levels of  $\beta$ -gal activity and massive accumulation of GM1 ganglioside throughout the CNS.<sup>4</sup>

GM1 gangliosidosis mice (4–6 per sex per group) were injected bilaterally into the thalamus ( $2 \times 2.2 \mu\text{L}$ ) or unilaterally into the lateral ventricle ( $14.8 \mu\text{L}$ ) with increasing doses of AAVrh.10-m $\beta$ gal (thalamus:  $3.5 \times 10^9$ ,  $1.0 \times 10^{10}$ ,  $3.5 \times 10^{10}$ ,  $1.0 \times 10^{11}$  vg/animal; i.c.v.:  $3.5 \times 10^{10}$ ,  $1.0 \times 10^{11}$ ,  $3.5 \times 10^{11}$  vg/animal). Mice were injected at 6–8 weeks of age and euthanized 1 month post injection, and tissues were collected for biochemical and histological analysis. Potential toxicity was also assessed by histopathologic analysis of brain sections.

Quantitative assays were performed to measure  $\beta$ -gal enzyme activity and GM1 ganglioside content in the brain, cerebellum, and spinal cord. Results presented in Figure 1 indicate that bilateral thalamic injection of AAVrh.10-m $\beta$ gal produced significant and dose-dependent increases in  $\beta$ -gal enzymatic activity and decrease of GM1 ganglioside content across all brain areas following thalamic injections. A less clear dose response was observed following i.c.v. administration of AAVrh.10-m $\beta$ gal. The lowest dose of  $3.5 \times 10^9$  vg used in intrathalamic delivery led to a significant increase of  $\beta$ -gal activity that approached or exceeded normal levels in the brain, indicating that a minimum effective dose was not reached. i.c.v. delivery (mid and high doses) resulted in comparable  $\beta$ -gal enzyme activity and GM1 ganglioside levels in the cerebellum and higher enzyme activity and storage correction in the spinal cord compared with intrathalamic injection. However, the maximum i.c.v. dose was 3.5-fold higher than the top intrathalamic dose. Also, the maximum i.c.v. dose ( $3.5 \times 10^{11}$  vg) was needed to achieve a reduction in cerebral GM1 ganglioside content similar to that achieved by intrathalamic injection at the lowest dose.

Histochemical staining with X-gal (Figure 2) showed a dose-dependent increase of  $\beta$ -gal enzyme activity in the brain of AAVrh.10-m $\beta$ gal-injected animals. Intense staining and distribution radiating from the thalamic injection site were observed. After i.c.v. injection, even at the highest dose, staining was much less intense but seemed more broadly distributed, reaching areas that were not stained after thalamic injection, such as the cerebellum.

	Thal	ICV
PBS		
3.5E+09		NA
1.0E+10		NA
3.5E+10		
1.0E+11		
3.5E+11	NA	

**Figure 2. Spatial distribution of  $\beta$ -gal enzyme in the mouse CNS at 1 month**  
Distribution of enzyme was assessed by histochemical staining with X-gal at acidic pH (blue stain) in sagittal sections of brain. Dose groups (expressed in viral genome) are indicated in the left column. Thal, thalamic injection; ICV, intracerebroventricular injection; NA, not applicable.

Direct intrathalamic injection, but not i.c.v. injection, resulted in dose-dependent toxicity at the two highest doses ( $3.5 \times 10^{10}$  vg and  $1.0 \times 10^{11}$  vg), consisting in mononuclear cell infiltrates in the thalamus with minor extensions into adjacent brain regions, especially the superior colliculus and caudate/putamen. At the highest dose, this was associated with neuronal loss near the site of injection (Figure S1).

In summary, this mouse study shows that i.c.v. injection of AAVrh.10-m $\beta$ gal, but not intrathalamic injection, can result in widespread (cerebrum, cerebellum, and spinal cord) correction of storage defects at a dose that is free of observable adverse effects. It is expected that this biochemical normalization of GM1 ganglioside metabolism in the CNS of GM1 mice would be associated with clinical improvement, as previous studies showed that lower levels of  $\beta$ -gal activity

restoration in the CNS were associated with phenotypic amelioration and extension of lifespan.<sup>9,11</sup>

#### Cat study

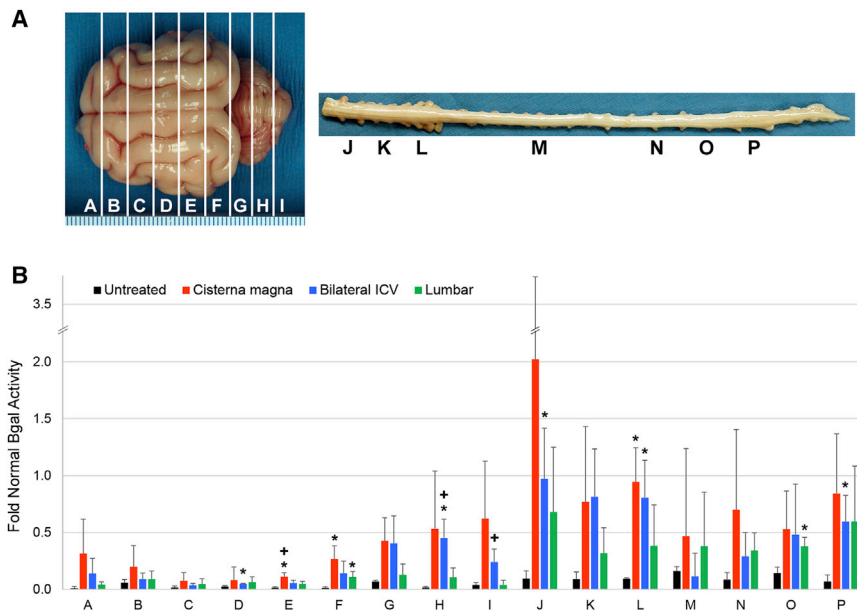
Naturally occurring feline GM1 gangliosidosis recapitulates the human late-infantile-onset disease in terms of enzymatic deficiency, storage levels, and CNS and peripheral organ pathology.<sup>13</sup> Various routes of CSF delivery of a feline version of LYS-GM101 were evaluated in GM1 gangliosidosis cats for their potential to impact CNS distribution and  $\beta$ -gal enzyme levels and associated storage reduction.

AAVrh.10-f $\beta$ gal was delivered to GM1 gangliosidosis cats via one of three routes: i.c.m. (n = 4, both sexes), i.c.v. (n = 4, both sexes), or i.t.l. (n = 4, both sexes). A total dose of  $1.0 \times 10^{12}$  vg/kg body weight was chosen for this study, based on the rationale that a relatively low dose would be most effective at revealing subtle differences in vector delivery across routes. Cats were treated at 2–5 months of age and euthanized at 1 month post injection. Untreated GM1 gangliosidosis cats (n = 4, both sexes) and wild-type (WT) cats (n = 4, both sexes) were used as controls.

For biochemical analysis, the brain and the spinal cord were collected and divided as shown in Figure 3A. Quantitative assay was performed to measure  $\beta$ -gal enzyme activity in homogenates of each of the blocks from the cerebrum, cerebellum, and spinal cord.  $\beta$ -gal enzyme activity was expressed as “fold normal” levels by dividing  $\beta$ -gal enzyme activity in each CNS block from treated animals by that in the corresponding block from normal (WT) animals. Results presented in Figure 3B indicate that bilateral i.c.v. and i.c.m. infusions of AAVrh.10-f $\beta$ gal produced elevations in  $\beta$ -gal enzyme activity in cerebrum, cerebellum, and spinal cord relative to untreated GM1 gangliosidosis cat tissues. While i.t.l. delivery produced elevations in  $\beta$ -gal enzyme activity in spinal cord, this route was ineffective at delivering  $\beta$ -gal to the cerebrum and cerebellum. In general, the highest  $\beta$ -gal enzyme activity in both the brain and spinal cord resulted from i.c.m. infusion, ranging from 0.08- to 0.62-fold normal (WT) levels in the brain and 0.47- to 2.0-fold normal levels in the spinal cord. Although no statistical difference in  $\beta$ -gal activity existed between i.c.m. and i.c.v. delivery routes, i.c.m. produced the highest mean  $\beta$ -gal activity in 15 of the 16 blocks of the CNS.

$\beta$ -gal activity was also measured in peripheral organs (data not shown), where the highest level was measured in the liver, with mean values similar across injection routes and ranging from 0.72- to 1.1-fold normal. In addition, heart  $\beta$ -gal activity showed significant elevations after treatment by i.c.m. (0.45-fold normal) or i.c.v. (0.32-fold normal) routes, with no elevation after i.t.l. injection. The presence of vector genomes (data not shown) and increased  $\beta$ -gal activity in peripheral organs indicates that vector can pass from the CSF to the blood and then transduce peripheral organs.

Filipin is an antibiotic polyene that can be used as a histochemical marker for GM1 ganglioside.<sup>14</sup> To evaluate lysosomal storage, filipin staining of the CNS was performed in a subset of treated GM1



**Figure 3. β-gal enzyme activity in the cat CNS at 1 month**

(A) At necropsy, the brain was cut into 6-mm blocks from the frontal pole through caudal cerebellum for a total of nine blocks (A–I). Spinal cord was removed in its entirety, and seven regions were assayed (J–P). (B) β-gal activity was analyzed in these CNS blocks and expressed as “fold of normal” activity, meaning that β-gal enzyme activity in each CNS block from treated animals was standardized to levels in the corresponding block from normal animals ( $n = 3$ ). Statistical significance was determined using a two-tailed t test. Symbols denote  $p < 0.05$  compared with the following groups: untreated GM1 gangliosidosis cats (\*); lumbar cisterna treated cats (+). No significant differences in β-gal activity existed between cisterna magna and i.c.v. injection routes.

gangliosidosis cats (Figure 4). Visualized as punctate white or light-gray dots, filipin staining is absent in the gray matter of the normal cat CNS, while prominent staining is observed in the gray matter of the cerebrum, cerebellum, brainstem, and spinal cord of untreated GM1 gangliosidosis cats. Filipin staining was diminished in the lumbar spinal cord of AAVrh.10-βgal-treated GM1 gangliosidosis cats, demonstrating partial clearance of storage material in all treated cats, regardless of the route of injection. Cats treated by i.c.m. injection had the most effective clearance in the cerebellum and brainstem, with partial clearance in the cerebrum, although variability existed across cats. The cerebrum, cerebellum, and brainstem were less effectively cleared of storage material in cats treated by the i.c.v. or lumbar routes in this study.

In summary, this study shows that CSF administration of AAVrh.10 vectors in a large animal model of GM1 gangliosidosis can provide widespread CNS delivery of β-gal. Despite a limited increase in enzyme activity at  $1.0 \times 10^{12}$  vg/kg, especially in the brain, it appeared that i.c.v. and i.c.m. administration are preferable over lumbar delivery in elevating β-gal activity in the brain. The highest β-gal enzyme activity and associated clearance of storage in both the brain and spinal cord resulted from i.c.m. infusion.

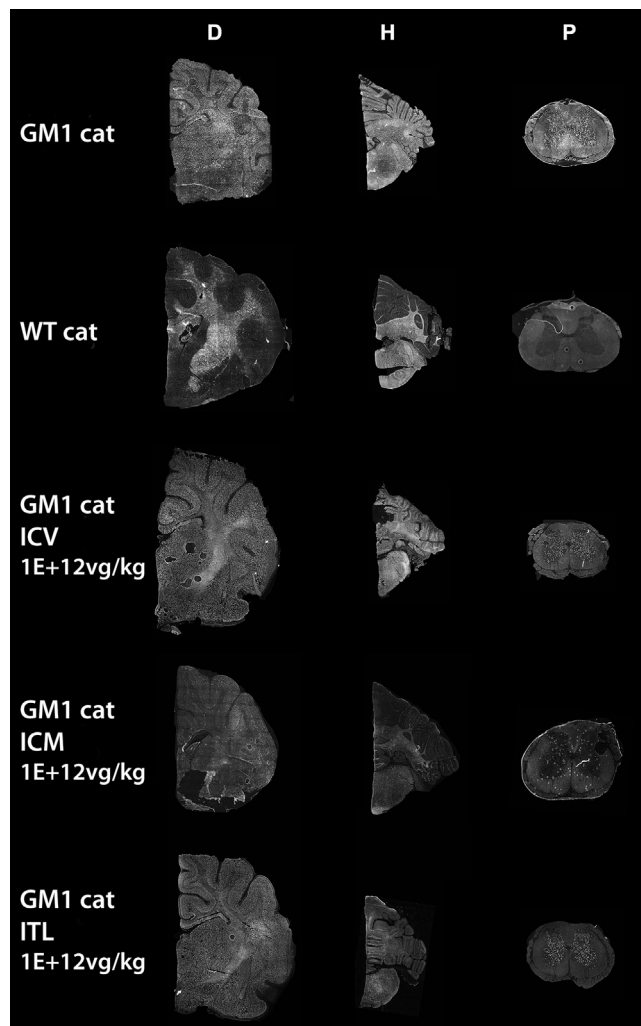
#### NHP study

NHPs were selected as the animal species for a GLP toxicity and biodistribution study and to identify an appropriate dose for the first-in-human clinical trial. Young animals between 2 and 3 years old at the time of administration were used in this study, which is within the childhood period of this species. The maximum feasible dose of LYS-GM101 (i.e.,  $5.4 \times 10^{13}$  vg) and a 4-fold lower dose (i.e.,  $1.4 \times 10^{13}$  vg) were tested via the i.c.m. route, and animals were sacrificed 3 or 6 months after treatment according to the design described in Table 1.

GLP biodistribution analysis of LYS-GM101 was performed in high-dose-injected animals for both 3-month and 6-month cohorts (Figure S2). At month 3, the vector LYS-GM101 was detected in all tissues and fluids tested. Highest amount of vector was present in the liver and in organs related to the injection site (brain, nervous system, and special sense system). Statistically significant differences in vector copy numbers were observed between males and females in the brain, with higher vector copy numbers in females. On average, females had 3-fold higher numbers of vector genomes in the brain than males ( $p = 1.40 \times 10^{-9}$ , t test). After 6 months vector was still present in all tissues, except thymus, in both males and females. Low levels of vector were also detected in testis and ovaries, with lower amounts at month 6 versus month 3. RNA copies of the LYS-GM101 vector were found in all tissues that were positive for the presence of the transgene DNA (data not shown).

To investigate whether the vector and transgene product were homogeneously distributed throughout the brain, the brain of each NHP was cut into 4-mm-thick slices, and even slabs were divided into  $10 \times 10$ -mm sections. Each section was divided in half, one of which was submitted for DNA quantification (month-3 cohort only) and the other for β-gal enzyme activity (both month-3 and month-6 cohorts). As illustrated in Figure 5, distribution of the vector genome was homogeneous throughout the 97–123 brain samples analyzed per animal.  $68\% \pm 16\%$  of analyzed samples in the high-dose group showed  $\geq 20\%$  increase of β-gal activity over background normal levels, indicating that β-gal activity increased throughout the brain rather than being limited to only a few brain areas. A global increase of enzyme activity was observed in the brain of both LYS-GM101-treated groups compared with the control group, with average 20% and 60% increases for the low- and high-dose group, respectively. The difference between treated and control groups was statistically significant at the high dose, with mean values of 83.4 and 52.1 nmol/h/mg, respectively ( $p = 0.002$ , t test).





**Figure 4. Filipin staining of storage material in the GM1 gangliosidosis cat CNS at 1 month**

Filipin staining appears as punctate white or gray dots in gray matter of untreated GM1 gangliosidosis cats, with little staining in gray matter of wild-type (WT) cats. Filipin staining was apparent in the cerebrum (block D located in Figure 3A) of all AAV-treated cats, with moderately diminished staining in the cat treated by cisterna magna (ICM) injection. Cerebellar gray matter and brainstem (block H located in Figure 3A) exhibited profound clearance of storage material after cisterna magna injection (with some variability between cats), but little clearance after bilateral intracerebroventricular (ICV) or intrathecal lumbar (ITL) infusions. Filipin staining was reduced in the lumbar intumescence of the spinal cord (block P located in Figure 3A) of all treated cats.

LYS-GM101 induced no mortality or any significant clinical signs, and there was no statistically significant change in body temperature, body weight, and qualitative food consumption in animals dosed with LYS-GM101 when compared with the control group and/or the pre-dose values. Immune monitoring consisted of assessment of the specific anti-AAVrh.10 and anti-human- $\beta$ -gal humoral responses in serum. In pre-dose samples, anti-AAVrh.10 immunoglobulin G

**Table 1. GLP toxicology and biodistribution study design in nonhuman primates**

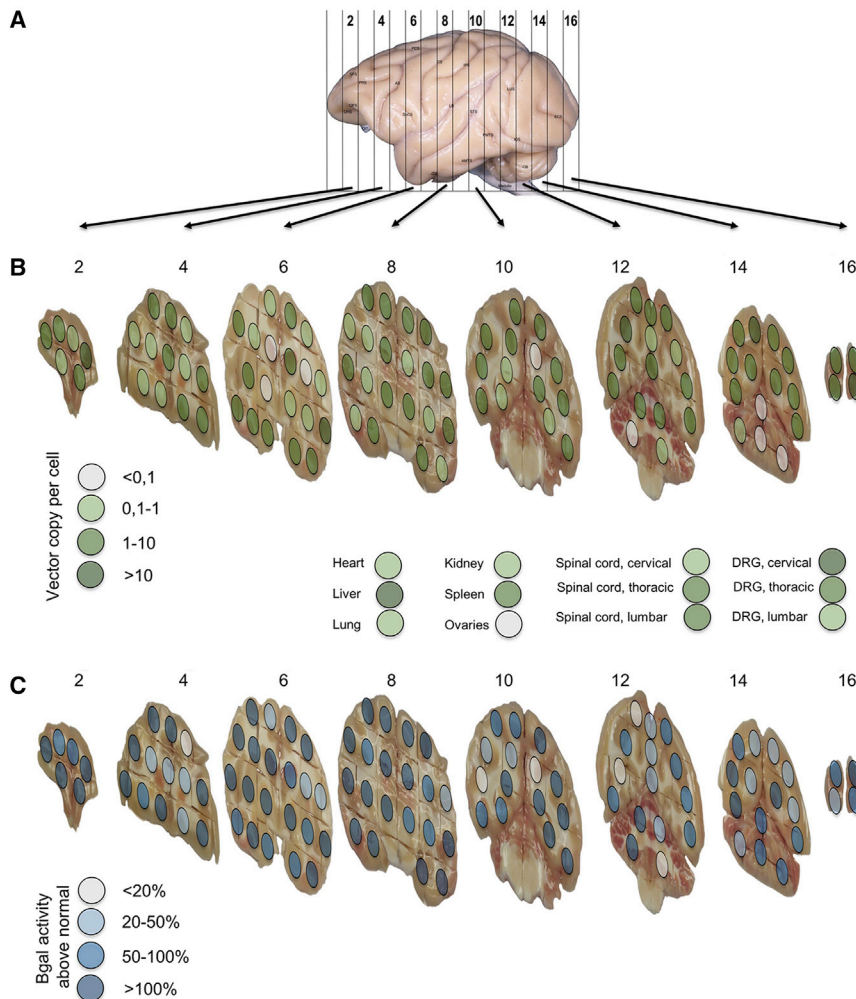
Treatment	Control (group 1)		Low dose (group 2)		High dose (group 3)		Total
	M	F	M	F	M	F	
Sacrifice at month 3 (day 78/79)	2	2	3	3	3	3	16
Sacrifice at month 6 (day 181/182)	1	1	0	0	2	2	6
Total	3	3	3	3	5	5	22

M, male; F, female (25–33 months of age).

LYS-GM101 or its vehicle was administered in one single session in the cisterna magna space by infusion of 4.5 mL at a flow rate of 0.5 mL/min at the following concentrations. Low dose:  $3.0 \times 10^{12}$  vg/mL, i.e.,  $1.4 \times 10^{13}$  vg/animal; high dose:  $1.2 \times 10^{13}$  vg/mL, i.e.,  $5.4 \times 10^{13}$  vg/animal.

(IgG) antibodies were detected in the serum of 19 of 22 (86.4%) animals before injection, regardless of the group, with titers comprised between 1:10 and 1:10,240. No correlation was observed between the AAVrh.10 antibody titer in the serum before vector injection and the level of  $\beta$ -gal activity increase in the CNS after vector injection (data not shown). After LYS-GM101 administration, anti-AAVrh.10 IgG antibodies were detected in the serum of all treated animals with titers  $\geq 1:10,240$ , whether they were negative or positive before injection. The titers of anti-AAVrh10 IgG at animal euthanasia showed a marked increase compared with pre-dose samples in already positive animals. Finally, there was no apparent correlation between antibody titers and vector dose. These data indicate that a humoral response against the vector capsid is observed following i.c.m. injection of LYS-GM101 in NHPs, confirming systemic exposure to the vector. No anti-human- $\beta$ -gal IgG antibodies were detected in samples of the control group or before LYS-GM101 administration. After LYS-GM101 administration, anti-human- $\beta$ -gal IgG antibodies were detected in serum of all treated animals with comprised titers between 1:40 and 1:10,240, with no vector dose-dependent relation. These data indicate that a humoral response against the transgene product occurred following i.c.m. injection of LYS-GM101 in NHPs. This humoral response was not unexpected, as the LYS-GM101 transgene codes for human  $\beta$ -gal, which shares only 94% identity with NHP  $\beta$ -gal (NCBI Reference Sequence: *Homo sapiens* NP\_000395.3 versus *Macaca fascicularis* NP\_001306360.1). No correlation was observed between the anti-human- $\beta$ -gal antibody titer in the serum and the level of  $\beta$ -gal activity increase in the CNS (data not shown).

The histopathology examination revealed adverse changes in the spinal cord and dorsal root ganglia in both sexes and at both dose levels (except in low-dose females), unrelated to dose, affecting sensory pathways, and consisting of up to marked vacuolation and gliosis of spinal nerves (cauda equina, dorsal segments); minimal to moderate vacuolation and axonal necrosis in the white matter (dorsal funiculi) at all spinal cord anatomical levels; a low incidence of various combinations of low severity neuronal necrosis, gliosis, and mononuclear cell infiltration in dorsal root ganglia; and minimal to slight axonal degeneration in sciatic nerves (Figure S3 and Table S1). These



**Figure 5. Vector and enzyme activity biodistribution in NHP brain**

Representative NHP injected with 4.5 mL of LYS-GM101 into the cisterna magna at a dose of  $1.8 \times 10^{13}$  vg/kg and analyzed after 3 months. (A) Left lateral view of an NHP brain with the location of the hemi-coronal brain slices shown. (B) qPCR analysis was performed using the PCR TaqMan method with primers and probe specific of the transgene, and results (color-coded with green dots) are expressed as mean vector copy per cell. (C) Enzyme activity analysis was performed as described in [materials and methods](#). Results (color-coded with blue dots) were expressed as percentage of endogenous activity determined as mean value of 431 brain punches from four vehicle-injected NHPs.

changes were present in similar incidence and severity at the high-dose level at month 3 or month 6, indicating absence of recovery or worsening ([Table S2](#)). Sensory tests performed prior to sacrifice at month 6 to evaluate conscious proprioceptive position, spinal and pannicular reflexes, and sensation did not reveal sensory deficits ([Table S3](#)).

## DISCUSSION

In the mouse model of GM1 gangliosidosis, administration of a murine analog of LYS-GM101 by the intrathalamic route led to high levels of  $\beta$ -gal activity in the brain of mice, associated with normalization of GM1 ganglioside storage as previously observed with AAV1.<sup>4</sup> However, the intrathalamic doses needed to provide therapeutic levels of  $\beta$ -gal and reduce storage defects in the cerebellum and the spinal cord were associated with histopathologic changes and neuronal loss at the injection site. Intrathalamic injection of an AAVrh8 vector expressing a related lysosomal enzyme ( $\beta$ -N-acetylhexosaminidase) in NHPs has been previously described to give rise to severe white and gray matter necrosis at the injection site that

was associated with clinical signs such as dyskinesia, ataxia, and loss of dexterity, with higher-dose animals eventually becoming apathetic.<sup>15</sup> Interestingly, such toxicity following intrathalamic injection of AAV observed in mice or NHPs was not reported after similar injection of AAV1 or AAVrh8 in GM1 cats, which led to high  $\beta$ -gal activity in the brain (up to 4.8-fold normal levels) associated with long-term biochemical and clinical correction of treated animals.<sup>5-7,16</sup>

Unlike the intrathalamic approach, no toxicity was observed in GM1 gangliosidosis mice following i.c.v. injection even at the highest dose ( $3.5 \times 10^{11}$  vg) that was associated with partial or complete biochemical normalization in all CNS compartments. Similar levels of  $\beta$ -gal activity increase were observed in

the brain of GM1 mice following i.c.v. injection of an AAVh68.Ubc.hGLB1 vector at a similar dose, which was associated with substantial correction of the disease phenotype and increased survival.<sup>9</sup> Comparison of several CSF routes of administration in the larger GM1 gangliosidosis cat model confirmed the superiority of i.c.m. and i.c.v. over i.t.l. for cerebrum, cerebellum, and spinal cord targeting, as previously described in NHPs.<sup>17,18</sup> Although i.c.m. and i.c.v. delivery gave similar distribution in the CNS, i.c.m. appears to carry less risk of immunity to the transgene product than i.c.v. administration, as observed in dogs, as well as a lower risk of procedure-related infections.<sup>19</sup>

These results in GM1 gangliosidosis animal models clearly established the qualitative principle that elevation of  $\beta$ -gal activity in the CNS is expected to lead to beneficial therapeutic effects in GM1 gangliosidosis. However, it is challenging to make quantitative extrapolations of effective human doses from those tested in animal disease models using vectors with potential species differences in transduction efficiency, potency, and specific enzyme activity. Instead, dose

selection for the clinical study was based on a target activity argument, under the assumption that therapeutic efficacy is a function of the level of  $\beta$ -gal activity in the CNS and that the latter can therefore be used to predict efficacy and select the therapeutic dose. The target  $\beta$ -gal activity in the CNS of GM1 gangliosidosis patients that would be expected to lead to therapeutic efficacy was estimated to be about 20% of normal, for the following reasons. First, there is a good correlation between residual enzyme activity and age of onset and severity of disease.<sup>2</sup> No disease is observed in carriers of GLB-1 mutations with greater than 10% residual enzyme activity. Consistently, asymptomatic heterozygote subjects have a mean of 36%–38% of normal  $\beta$ -gal activity with a lower limit of 16%–19%.<sup>20</sup> Although carriers have consistent levels of enzyme activity in each cell versus the potential for cell-to-cell variability produced by gene therapy, an average of 20% normal is a reasonable target when distribution is relatively uniform. Second, Sandhoff and colleagues,<sup>21–23</sup> using an enzyme kinetic model of lysosomal substrate turnover, demonstrated that only when enzyme activity decreases below a critical threshold, which is between 5% and 20% of normal for many different lysosomal enzymes, will substrates accumulate and lead to lysosomal storage pathology. Importantly, pre-clinical studies in GM1 gangliosidosis animal models confirm the notion of the  $\sim$ 20% threshold. In GM1 gangliosidosis mice, restoration of 10%–20% of normal  $\beta$ -gal activity in the brain is sufficient to achieve significant biochemical impact with phenotypic amelioration and extension in lifespan,<sup>11</sup> and restoration of brain  $\beta$ -gal activity to 2- to 3-fold lower levels than in heterozygotes produced beneficial effects on neurological scores, lysosomal pathology, and survival.<sup>9</sup>

Clinical dose selection was therefore based on a GLP study in NHPs, a more relevant model for volume and dose extrapolations to human CNS, using the clinical LYS-GM101 vector. NHP brains are 150-times and 3-times larger than murine and feline brains, respectively, with a CNS architecture and organization that more closely resembles the human brain. A global increase of  $\beta$ -gal activity was observed in NHP brain 3 months after i.c.m. injection of LYS-GM101 at  $1.0 \times 10^{12}$  vg/mL of CSF and  $4.0 \times 10^{12}$  vg/mL of CSF, with 20% and 60% increases compared with vehicle-treated animals, respectively. This magnitude of average  $\beta$ -gal activity increase, together with a broad enzyme distribution throughout the brain, namely 68% of analyzed brain samples from the high-dose group with  $\geq 20\%$  increase of  $\beta$ -gal activity over background levels, suggests that at similar doses in humans, LYS-GM101 should be able to elicit clinical improvements in patients with GM1 gangliosidosis.

While the vector and the transgene appeared to be broadly distributed in NHP brain, it is possible that this occurred in clusters rather than in even distribution over large populations of CNS cells. To gain additional information about the nature of transduced cell types (neurons, astrocytes, oligodendrocytes) and an estimation of the percentage of transduced cells in various areas, *in situ* hybridization and/or histochemical analysis of tissue sections at the cellular level would be required, which was beyond the scope of the current study. It should be pointed out however, that even relatively low levels of cellular

transduction may lead to considerable correction of lysosomal pathology, due to the phenomenon of cross-correction whereby lysosomal enzymes are secreted from producing cells and taken up by neighboring cells, e.g., via mannose-6-phosphate receptor-mediated transport.<sup>24</sup> As a consequence, the spread of  $\beta$ -gal activity will likely go beyond the spread of the vector itself, even if transduction occurs in clusters rather than in a uniform manner across the tissue.

GLP biodistribution analysis showed the highest amount of vector in the liver and  $\sim$ 10-fold lower levels found in the CNS, as observed in other NHP studies after i.c.m. delivery of AAV vectors.<sup>25,26</sup> Transduction of peripheral organs, also observed in GM1 cats, was expected, as vector can pass into the blood circulation following CSF injection.<sup>27</sup> Supplying  $\beta$ -gal to peripheral organs, especially liver and heart, could have a beneficial impact on somatic symptoms that can be associated with GM1 gangliosidosis, such as cardiomyopathy and hepatosplenomegaly.<sup>3</sup>

Drainage of the vector from the CSF into the periphery likely explains why NHPs dosed with LYS-GM101 mounted a humoral immune response against human  $\beta$ -gal, which shares 94% sequence identity with the cynomolgus monkey protein. Likewise, cross-reactive immunologic material (CRIM)-negative GM1 patients, i.e., individuals with biallelic nonsense mutations which do not express full-length  $\beta$ -gal protein, may mount a humoral immune response against the transgene product, including potentially neutralizing antibodies. This could potentially dampen or inhibit the therapeutic efficacy of LYS-GM101 in the periphery. However, since antibodies do not cross the blood-brain barrier,<sup>28</sup> anti- $\beta$ -gal antibodies would not be expected to impact the therapeutic efficacy of LYS-GM101 in the CNS. Consistent with this notion, no correlation was observed between anti-human- $\beta$ -gal antibody titer in serum and the extent of  $\beta$ -gal activity increase in the CNS of NHPs.

Histopathologic examination revealed adverse changes in the sensory pathways of the spinal cord and dorsal root ganglia in both sexes, at both dose levels and unrelated to dose. These changes were present in similar incidence and severity at the high-dose level at month 3 or month 6, indicating absence of recovery or aggravation. Importantly, no clinical signs were observed in animals of the 3-month or 6-month cohorts, including additional sensory function tests in the 6-month cohort. Similar asymptomatic vector-induced microscopic changes in sensory pathways were previously described in toxicology studies in NHP following AAV vector administration into the blood or CSF.<sup>18,25–27,29</sup> Dorsal root ganglia (DRG) neurons in monkeys and pigs seem to be more sensitive to AAV-induced DRG toxicity than other species.<sup>26</sup> Importantly, a recent study demonstrated the absence of sensory microscopic findings 3 years and 8 months after intrathecal cervical administration to 1-month-old rhesus monkeys of the same AAV9 vector that previously caused toxicity in adult rhesus monkeys.<sup>30</sup> These results suggest that infant monkeys may be less prone to injury of DRG neurons, or that repair may be more efficient in infants and/or could potentially occur after a period not captured in the 6-month study in adult NHPs. The mechanism responsible for

histopathologic findings observed in the NHP study is unknown but could be associated with high transgene expression in sensory neurons.<sup>31</sup> DRG neurons are highly transduced after intra-CSF delivery of AAV vectors,<sup>25,26</sup> a finding confirmed in our NHP study with up to  $4.9 \times 10^6$  vg/ $\mu$ g of DNA and up to  $2.3 \times 10^8$  vg/ $\mu$ g of RNA found in high-dose LYS-GM101 treated animals. Interestingly, no vector-related histopathology was apparent in spinal cord, DRG, and sciatic nerve sections from GM1 gangliosidosis cats 10 months after treatment with the feline analog of LYS-GM101 via the i.c.m. route at a dose similar to the highest dose tested in NHPs ( $1.5 \times 10^{13}$  vg/kg) (unpublished data). Similarly, no sensory neuron toxicity was reported in mucopolysaccharidosis type I cats that were treated via i.c.m. injection of AAV9 carrying the feline  $\alpha$ -L-iduronidase (IDUA)<sup>32</sup> gene at doses similar to those associated with DRG toxicity in NHPs using AAV9 carrying human IDUA.<sup>26</sup> Use of species-specific transgene in dogs was also not associated with the CNS inflammation previously observed using human transgene after injection of AAV9 into the CSF.<sup>33,34</sup> These observations suggest that cats and dogs may be less sensitive to AAV vector-induced DRG toxicity or that the toxicity observed in NHPs may be related to the use of a foreign (human) transgene in the NHP study. In support of the latter hypothesis, spinal cord and DRG abnormalities have been reported in toxicology studies in NHPs using combined systemic and intrathecal administration of a human frataxin (FXN)-encoding AAV9 vector, whereas no abnormalities were found in two NHPs treated with a similar dose of a cynomolgus-specific FXN-encoding vector.<sup>35</sup>

Even though the histopathologic findings observed with LYS-GM101 in NHPs were asymptomatic, they warrant careful monitoring for signs of sensory neuron toxicity in the first-in-human P1-GM-101 clinical trial ([ClinicalTrials.gov](https://clinicaltrials.gov/ct2/show/study/NCT04273269) identifier: NCT04273269) that was recently initiated to assess the safety and efficacy of LYS-GM101 in children with GM1 gangliosidosis. Even though T cell responses against the transgene product were not analyzed in the NHP toxicology study, histology did not reveal signs of cytotoxic immune responses. Nevertheless, to mitigate against potential T cell-mediated toxicity, immune suppression is used in the clinical trial. The dose of LYS-GM101 tested in the clinical trial, which is 2-fold lower than the high dose tested in NHPs (i.e.,  $2.0 \times 10^{12}$  vg/mL of CSF), is expected to restore greater than 20% of normal  $\beta$ -gal activity in the brain and spinal cord of patients with GM1 gangliosidosis. As discussed above, this level of restoration of enzyme activity is predicted to have a significant positive impact on disease progression. Even supplying just a few percent of normal activity to a patient with type I GM1 gangliosidosis could be beneficial, since this most severe form of the disease, with a life expectancy of 2–3 years, is associated with less than 1% residual activity, while the relatively milder juvenile and adult forms of disease are associated with 3%–10% of residual activity.<sup>2</sup>

## MATERIALS AND METHODS

### Mice

GM1 gangliosidosis (GM1) mice were obtained from Dr. Alessandra d'Azzo (St. Jude Children's Research Hospital, Memphis, TN) and

have been described previously.<sup>12</sup> The mouse study was conducted at University of Massachusetts Chan Medical School (Worcester, MA) with ethical committee approval in accordance with the National Institutes of Health Guide for the Care and Use of Laboratory Animals.

### Cats

GM1 cats<sup>13</sup> are bred and maintained at Auburn University (Auburn, AL) where the study took place, and its Institutional Animal Care and Use Committee approved the research described herein.

### Nonhuman primates

Healthy cynomolgus monkeys (*Macaca fascicularis*) (between 26 and 33 months old on the day of the randomization) were received from Nafovanny (Vietnam). The nonhuman primate (NHP) study was conducted at ERBC (Baugy, France) in compliance with the guidelines concerning GLP dated March 14, 2000 published by the French Ministry of Social Affairs and National Solidarity, State Secretariat for Health, which are in accordance with the Directive 2004/10/EC and are accepted by the US Food and Drug Administration and Japanese authorities. This study was undertaken in accordance with the Directive 2010/63/UE of the European Parliament and Council of September 22, 2010 for the protection of animals used for scientific purposes.

### AAV production

LYS-GM101 is a recombinant AAV.rh10 vector that carries AAV2 inverted terminal repeats flanking a transgene cassette with the human WT GLB1 gene cDNA driven by cytomegalovirus enhancer fused to a chicken  $\beta$ -actin promoter/rabbit  $\beta$ -globin intron (CAG promoter), and a human growth hormone polyadenylation signal.

The mouse and feline analogs (AAVrh.10-m $\beta$ gal and AAVrh.10-f $\beta$ gal) of LYS-GM101 containing the WT murine or feline GLB1 cDNA, respectively, were produced at UMass Medical School, Gene Therapy Center (Worcester, MA) by transient transfection of HEK293 cells and purified by iodixanol ultracentrifugation as previously described.<sup>36</sup>

An engineering batch of LYS-GM101 using a process similar to clinical good manufacturing practices, supplied by Brammer Bio PD Lab (Alachua, FL), was used for the GLP study in NHP. The batch was produced using a triple transfection process in adherent hyperstack-36 and purified through affinity chromatography before being concentrated and formulated into final formulation buffer (PBS + 0.001% Pluronic) at target concentration. Titration was performed using a qPCR assay designed to target the transgene.

### Delivery of AAV vector

Six- to eight week-old GM1 mice were anesthetized by intraperitoneal injection of ketamine (125 mg/kg) and xylazine (12.5 mg/kg) in 0.9% saline, and placed in a small animal stereotaxic frame (Stoelting, Wood Dale, IL). An incision was made over the skull, the periosteum was removed, and a burr hole was made at the appropriate stereotaxic



coordinates using a high-speed drill (Dremel, Racine, WI). The infusions were performed with sterile glass Hamilton syringes fitted with 33-gauge needles using an UltraMicroPump system (World Precision Instruments, Sarasota, FL). AAVrh10-mβgal vector was infused bilaterally into the thalamus (2.22 μL per site; 0.2 μL/min) or by single 14.8 μL i.c.v. infusion (0.5 μL/min). Vector solution was diluted with PBS without calcium or magnesium (Invitrogen) to reach the different tested doses. In the control groups, age-matched GM1 mice received the same infusion of PBS into the thalamus or i.c.v. infusion (same volume as above). The needle was left in place for 2.5 min after the injection was finished and then retracted halfway and left in place for an additional 2.5 min before complete withdrawal. The incision was closed with surgical staples or collodion, and the animal was allowed to recover completely before being returned to the holding room.

Two- to five-month-old GM1 cats were injected with AAVrh10-fβgal vector via i.c.m. (n = 4, both sexes), i.c.v. (n = 4, both sexes), or i.t.l. (n = 4, both sexes) injection at a dose of  $1.0 \times 10^{12}$  vg/kg body weight. Because individual cat weights varied, the total doses also varied and were calculated based on body weight. Anesthesia was induced with ketamine (10 mg/kg) and dexmedetomidine (0.04 mg/kg) through an intravenous catheter and maintained using isoflurane (0.5%–1.5%) in oxygen delivered through an endotracheal tube. Vector titer was held constant, so injected volume varied with the weight of the animal. Bilateral i.c.v. delivery was performed essentially as previously described<sup>37</sup> by injecting each lateral ventricle with 130–290 μL of vector at ~25–50 μL/min. For i.c.m. injections the cisterna magna was located by palpation, and needle placement was confirmed by withdrawal of CSF. Vector volumes of 225–850 μL were delivered at ~25–50 μL/min. i.t.l. injection was performed at the level of the caudal lumbar vertebrae with 300–700 μL of vector delivered at 50–100 μL/min.

NHPs (26–33 months old) were injected with LYS-GM101 or vehicle in one single session using a 20-gauge spinal needle manually inserted by palpation into the cisterna magna space of anesthetized animals. Correct positioning was confirmed by the flow of CSF from the needle. The location of the needle was secured using a stereotaxic frame. The needle was connected to an infusion pump through an extension set of 1 m to allow infusion of 4.5 mL of test item or vehicle at a flow rate of 0.5 mL/min. At the end of the injection, the needle was left in place for 5 min to prevent back reflow. The needle was then removed, and pressure was applied for about 30 s to the injection site.

#### Necropsy and sample processing

One month after injection, mice were sacrificed by an overdose of ketamine/xylazine (Fort Dodge Animal Health, Fort Dodge, IA and Lloyd Laboratories, Shenandoah, IA), cleared by transcardiac perfusion with ice-cold PBS, and harvested according to assay needs. Tissues were collected for biochemical and histological analysis.

At necropsy, cat brain was cut into 6-mm blocks from the frontal pole through caudal cerebellum, for a total of nine blocks (parts A–I in Fig-

ure 3A). From each block, the right hemisphere was frozen in OCT medium for enzyme assays, and the left hemisphere was further cut in half and stored in 10% formalin (rostral half) or frozen in liquid nitrogen and stored at  $-80^{\circ}\text{C}$  (caudal half). The spinal cord was removed in its entirety, and seven regions were assayed (parts J–P in Figure 3A). The spinal cord was stored in OCT for enzyme assays or 10% formalin, or frozen in liquid nitrogen for storage at  $-80^{\circ}\text{C}$ .

On the day of necropsy and after an overnight fast prior to sacrifice, NHPs were pre-medicated with ketamine HCl and euthanized by subtotal exsanguination following administration of sodium pentobarbital anesthesia by the intravenous route. Organs/tissues selected for enzyme activity and/or DNA quantification were collected from all animals at the pre-defined endpoints at 3 and 6 months after infusion. For paired organs and depending on the size, one side was sampled to assess for biodistribution and DNA quantification of vector genomes, and the remaining tissues and/or the other side were sampled for histopathologic examination. For single organs (except for the brain), only a part of the organ was sampled for DNA quantification, the other part being sent for histopathologic examination. Brain (perfused with cold sterile saline) was cut into 4-mm-thick coronal slices using a brain slicer. Odd slabs were fixed in buffered formalin for histopathology examination. Even slabs were divided into  $10 \times 10$ -mm sections and photographed (with scale) to document the location of each section. Each section was divided in half, one submitted for DNA quantification was used for biodistribution analysis and the other for β-gal enzyme activity (3-month cohort only).

#### β-gal activity assay

Cat tissues were evaluated as described previously.<sup>7</sup> Mice and NHP tissues were homogenized in four volumes of water, followed by three cycles of freeze-thawing and centrifugation at  $1,000 \times g$  for 5 min at  $4^{\circ}\text{C}$ . Supernatants were assayed for β-gal activity using 4-methylumbelliferyl-β-D-galactopyranoside in a microplate fluorimetric assay<sup>38</sup> and represented as nmol/h/mg protein.

β-gal enzyme activity in CNS samples of NHP was measured in 99–128 brain samples and three spinal cord samples per animal. The level of β-gal enzyme activity observed in vehicle-treated animals corresponds to the endogenous activity of the enzyme in NHP and was considered as the background level in animals injected with LYS-GM101. In vehicle-treated animals, the mean enzymatic activity in the brain was 52.1 (SD = 4.3; n = 4) nmol/h/mg of protein, with no significant difference between sexes or time cohorts.

#### Vector copy number

The following tissues from NHPs injected with LYS-GM101 at the higher dose (at both 3- and 6-month endpoints) were analyzed for vector genome copy number by qPCR. DRG and spinal cord at three levels (cervical, thoracic, and lumbar), vagus nerve, heart, lungs with bronchi, liver, thymus, spleen, lymph nodes (mesenteric and mandibular), kidney, ovary, or testis from NHPs injected with LYS-GM101 at the higher dose were analyzed for vector genome copy number by qPCR at both 3 months and 6 months. Genomic DNA was extracted

using a NucleoSpin Tissue kit (Macherey-Nagel). Analysis of vector biodistribution was performed by quantitative TaqMan PCR. For quantification of AAV vector copy numbers, a standard curve was prepared by adding specific amounts of linearized LYS-GM101 plasmids. Quantification of endogenous gene  $\beta$ 2-microglobulin was used to monitor the potential inhibitory effect of tissues on qPCR reaction. The primer sequences used to quantify AAV vector copy numbers were forward 5'-GTT CGG CTT CTG GCG TGT G-3', reverse 3'-AGG ATG CGA ACC AGG AAC CC-5', and probe sequence 5'-CCT ACA GCT CCT GGG CAA CGT GCT GGT-3'. Results originally expressed as vector copy per microgram of DNA were converted into vector copy per cell for brain sample mapping considering a genome median total genome length per cell of 2,946.84 Mb for *Macaca fascicularis*.

### GM1 ganglioside analysis

GM1 ganglioside content in the CNS was measured by liquid chromatography-tandem mass spectrometry at the University of Massachusetts Medical School Proteomics and Mass Spectrometry Facility. In brief, 0.04 or 0.1 mg/ $\mu$ L of tissue homogenate was diluted in 0.01 M phosphate citrate buffer with 0.1% Triton X-100 (VWR) (pH 4.4) to 25 or 50  $\mu$ L, respectively. Each sample was spiked with 3,000 ng of d3-labeled GM1 ganglioside formulated in methanol (Matreya, State College, PA). Standard calibration curves were made with GM1-ganglioside formulated in methanol (Matreya) over the range of 200–5,000 ng in phosphate citrate buffer with 0.1% Triton X-100, also spiked with 3,000 ng of d3-GM1 ganglioside and also put through the extraction process. Total lipids were extracted twice by vortexing and sonicating samples for 30 s with 1 mL of isopropanol/ethyl acetate/water (60:30:10), combining both supernatants after centrifugation at  $10,000 \times g$  for 10 min. Samples were dried and then resuspended in 100  $\mu$ L of buffer composed of 80% mobile phase A (0.1% [v/v] formic acid) and 20% mobile phase B (47.5% methanol, 47.5% isopropanol, 4.9% water, and 0.1% formic acid). For each sample, 2  $\mu$ L was injected in duplicate onto a  $2.1 \times 50$ -mm Kinetex (Phenomenex, Torrance, CA) C18 (1.7 $\mu$ , 100 Å) column using an Acquity high-performance liquid chromatography instrument (Waters, Milford, MA) coupled to a Quattro Premier XE (Waters) mass spectrometer operating in the negative ion electrospray mode. Gangliosides were eluted at 270  $\mu$ L/min using the following gradient: 0–1 min (80% B); 1–5 min (80%–100% B); 5–7 min (100% B); 7.1–12 min (80% B). Multiple reaction monitoring transitions for GM1 (fatty acids: 18:0, d3-18:0) were monitored by following corresponding (M-H)<sup>−</sup> precursor ions to the common sialic acid anion fragment at  $m/z$  290 (cone voltage, 90 V; collision energy, 70 eV; collision gas pressure, 2.2  $\mu$ bar). The area of GM1 18:0 lipid was normalized to the d3-18:0 GM1 lipid species internal standard. In brief, 14.8% of the area of 18:0 GM1 lipid was subtracted from the area of d3-18:0 GM1 to correct for d3-18:0 GM1/18:0 GM1 overlap. The ratio of the area of 18:0 GM1 to the corrected area of d3-18:0 GM2 was calculated and nanograms of GM1 lipid were determined from the standard curve. Total GM1 ganglioside concentrations were then normalized to total protein content in tissue homogenate, measured by QuickStart Bradford Protein Assay (Bio-Rad) with serial dilutions of BSA as protein standard.

### Histopathology

NHP tissues fixed in formalin were paraffin embedded, sectioned, and stained with H&E according to standard protocols. Tissues were evaluated histologically by a board-certified veterinary anatomic pathologist. The severity of lesions was graded as follows: grade 1 (minimal histopathologic change from inconspicuous to barely noticeable); grade 2 (slight histopathologic change that is noticeable but not prominent); grade 3 (moderate histopathologic change that is prominent but not a dominant feature); grade 4 (marked histopathologic change that is dominant but not an overwhelming feature); grade 5 (severe histopathologic change that is an overwhelming feature).

### Immunohistochemistry and histochemistry

For histological analyses in mice, fresh frozen sagittal brain and transverse spinal cords sections were cut at 20  $\mu$ m thickness on a cryostat (Thermo Fisher Scientific) at  $-12/-13^{\circ}\text{C}$  and stained as follows.  $\beta$ -gal enzyme in brain and spinal cord sections was assessed by 5-bromo-4-chloro-3-indolyl-D-galactosidase (X-gal) histochemical staining. Frozen sections were fixed for 10 min in 0.25% glutaraldehyde in PBS at room temperature followed by two washes in PBS. Sections were incubated overnight at  $37^{\circ}\text{C}$  in X-gal solution (5 mM  $\text{K}_4\text{Fe}(\text{CN})_6$ , 5 mM  $\text{K}_3\text{Fe}(\text{CN})_6$ , 2 mM  $\text{MgCl}_2$ , 1 mg/mL X-gal in PBS, pH 5.0). X-gal reacted sections were washed in PBS and counterstained with Nuclear Fast Red (Vector Laboratories, Burlingame, CA). Images of X-gal reacted hemispheres were acquired in a Nikon Supercoolscan 9000 slide scanner at 3,000 dpi. Nuclear Fast Red stained slides representing multiple step sections of the frozen mouse brain were transferred to Vet Path Services (Mason, OH) for microscopic evaluation by a board-certified pathologist.

For analysis of  $\beta$ -gal activity in cats, frozen sections at 40  $\mu$ m were thawed and fixed in 0.5% glutaraldehyde in citrate phosphate buffer (50 mM  $\text{Na}_2\text{HPO}_4 \cdot 7\text{H}_2\text{O}$ , 50 mM citric acid monohydrate, 10 mM NaCl), pH 4.2 (brain) or pH 5.2 (spinal cord), for 10 min followed by washes in citrate phosphate buffer. Tissue sections were then incubated at  $37^{\circ}\text{C}$  overnight in citrate phosphate buffer, pH 4.2 (brain) or pH 5.2 (spinal cord), containing 20 mM  $\text{K}_4\text{Fe}(\text{CN})_6$ , 20 mM  $\text{K}_3\text{Fe}(\text{CN})_6$ , 2 mM  $\text{MgCl}_2$ , 0.02% Igepal, 0.01% deoxycholic acid, and X-gal (2 mg/mL). On the next day sections were washed, dehydrated, and mounted.

Filipin staining in cats was performed essentially as described previously.<sup>8</sup> In brief, sections were fixed for 10 min in 4% paraformaldehyde followed by washes in PBS and a 10-min incubation in 1.5% glycine. After further washes in PBS, sections were incubated for 1 h at room temperature with filipin (0.05 mg/mL; Sigma, St Louis, MO), washed, and coverslipped with fluorescent mounting medium (DakoCytomation). Images were converted to grayscale for visualization.

### Serum anti- $\beta$ -gal and anti-AAV antibody analysis

Analysis was done by ELISA. In brief, Nunc MaxiSorp P96 plates (Sigma) were coated with recombinant  $\beta$ -gal protein (Origene) or

AAVrh10 particles. After saturation of the wells, samples were added at six dilutions (four fold dilutions from 1:10 to 1:10,240). After incubation with anti-Rhesus HRP antibody, TMB substrate was added and absorbance at 450 nm and 570 nm was measured.

### Statistical analysis

Data were analyzed by one-way analysis of variance or Student's t test to calculate statistical significance between animal groups using Statview 5.0 or Microsoft Excel software.

### DATA AVAILABILITY

All data and supporting material are available within the article and [supplemental information](#).

### SUPPLEMENTAL INFORMATION

Supplemental information can be found online at <https://doi.org/10.1016/j.omtm.2022.10.004>.

### ACKNOWLEDGMENTS

We thank Kimberley S. Gannon for her participation in the design and implementation of these studies. We thank the ERBC team for their help in the NHP GLP study, the Genosafe team for qPCR and  $\beta$ -gal enzyme activity analysis, the Gene Therapy Immunology Core team for the anti- $\beta$ -gal and anti-AAVrh10 antibody assays, and the Lysogene team for their continuous support and discussions.

### AUTHOR CONTRIBUTIONS

M.H., D.R.M., and M.S.-E. designed experiments, conducted formal data analysis, and wrote the manuscript. A.L.G., A.N.R., H.L.G.-E., J.A.H., S.T., and L.S. conducted the experiments. K.A., X.M., and L.G. contributed to the protocol development and provided expertise on experimental approaches. R.L. contributed to interpretation of the results and wrote the manuscript. All authors contributed to the editing of the manuscript.

### DECLARATION OF INTERESTS

These studies were funded by grants from Lysogene, who were also involved in study design. M.H., X.M., L.G., and R.L. are full-time employees and hold equity of Lysogene. M.S.-E. and D.R.M. are shareholders in Lysogene. M.S.-E., H.L.G.-E., A.N.R., A.L.G., and D.R.M. are beneficiaries of a licensing agreement with Sio Gene Therapies for a separate technology.

### REFERENCES

- Brunetti-Pierri, N., and Scaglia, F. (2008). GM1 gangliosidosis: review of clinical, molecular, and therapeutic aspects. *Mol. Genet. Metab.* *94*, 391–396.
- Regier, D.S., and Tiff, C.J. (2013). GLB1-Related Disorders, in *GeneReviews*(R), M.P. Adam, et al., eds.
- Regier, D.S., Proia, R.L., D'Azzo, A., and Tiff, C.J. (2016). The GM1 and GM2 gangliosidoses: natural history and progress toward therapy. *Pediatr. Endocrinol. Rev.* *13*, 663–673.
- Baek, R.C., Broekman, M.L.D., Leroy, S.G., Tierney, L.A., Sandberg, M.A., d'Azzo, A., Seyfried, T.N., and Sena-Esteves, M. (2010). AAV-mediated gene delivery in adult GM1-gangliosidosis mice corrects lysosomal storage in CNS and improves survival. *PLoS One* *5*, e13468.
- Gray-Edwards, H.L., Jiang, X., Randle, A.N., Taylor, A.R., Voss, T.L., Johnson, A.K., McCurdy, V.J., Sena-Esteves, M., Ory, D.S., and Martin, D.R. (2017). Lipidomic evaluation of feline neurologic disease after AAV gene therapy. *Mol. Ther. Methods Clin. Dev.* *6*, 135–142.
- Gray-Edwards, H.L., Maguire, A.S., Salibi, N., Ellis, L.E., Voss, T.L., Diffie, E.B., Koehler, J., Randle, A.N., Taylor, A.R., Brunson, B.L., et al. (2020). 7T MRI predicts amelioration of neurodegeneration in the brain after AAV gene therapy. *Mol. Ther. Methods Clin. Dev.* *17*, 258–270.
- McCurdy, V.J., Johnson, A.K., Gray-Edwards, H.L., Randle, A.N., Brunson, B.L., Morrison, N.E., Salibi, N., Johnson, J.A., Hwang, M., Beyers, R.J., et al. (2014). Sustained normalization of neurological disease after intracranial gene therapy in a feline model. *Sci. Transl. Med.* *6*, 231ra48.
- Broekman, M.L.D., Baek, R.C., Comer, L.A., Fernandez, J.L., Seyfried, T.N., and Sena-Esteves, M. (2007). Complete correction of enzymatic deficiency and neurochemistry in the GM1-gangliosidosis mouse brain by neonatal adeno-associated virus-mediated gene delivery. *Mol. Ther.* *15*, 30–37.
- Hinderer, C., Nosratabkhsh, B., Katz, N., and Wilson, J.M. (2020). A single injection of an optimized AAV vector into cerebrospinal fluid corrects neurological disease in a murine model of GM1 gangliosidosis. *Hum. Gene Ther.* *31*, 1169–1177.
- Gross, A.L., Gray-Edwards, H.L., Bebout, C.N., Ta, N.L., Nielsen, K., Brunson, B.L., Lopez Mercado, K.R., Osterhoudt, D.E., Batista, A.R., Maitland, S., et al. (2021). Intravenous delivery of adeno-associated viral gene therapy in feline GM1 gangliosidosis. *Brain* *145*, 655–669.
- Weismann, C.M., Ferreira, J., Keeler, A.M., Su, Q., Qui, L., Shaffer, S.A., Xu, Z., Gao, G., and Sena-Esteves, M. (2015). Systemic AAV9 gene transfer in adult GM1 gangliosidosis mice reduces lysosomal storage in CNS and extends lifespan. *Hum. Mol. Genet.* *24*, 4353–4364.
- Hahn, C.N., del Pilar Martin, M., Schröder, M., Vanier, M.T., Hara, Y., Suzuki, K., Suzuki, K., and d'Azzo, A. (1997). Generalized CNS disease and massive GM1-ganglioside accumulation in mice defective in lysosomal acid beta-galactosidase. *Hum. Mol. Genet.* *6*, 205–211.
- Baker, H.J., and Lindsey, J.R. (1974). Animal model: feline GM1 gangliosidosis. *Am. J. Pathol.* *74*, 649–652.
- Arthur, J.R., Heinecke, K.A., and Seyfried, T.N. (2011). Filipin recognizes both GM1 and cholesterol in GM1 gangliosidosis mouse brain. *J. Lipid Res.* *52*, 1345–1351.
- Golebiowski, D., van der Bom, I.M.J., Kwon, C.S., Miller, A.D., Petrosky, K., Bradbury, A.M., Maitland, S., Kühn, A.L., Bishop, N., Curran, E., et al. (2017). Direct intracranial injection of AAVrh8 encoding monkey beta-N-acetylhexosaminidase causes neurotoxicity in the primate brain. *Hum. Gene Ther.* *28*, 510–522.
- Gray-Edwards, H.L., Regier, D.S., Shirley, J.L., Randle, A.N., Salibi, N., Thomas, S.E., Latour, Y.L., Johnston, J., Golas, G., Maguire, A.S., et al. (2017). Novel biomarkers of human GM1 gangliosidosis reflect the clinical efficacy of gene therapy in a feline model. *Mol. Ther.* *25*, 892–903.
- Hinderer, C., Bell, P., Vite, C.H., Louboutin, J.P., Grant, R., Bote, E., Yu, H., Pukenas, B., Hurst, R., and Wilson, J.M. (2014). Widespread gene transfer in the central nervous system of cynomolgus macaques following delivery of AAV9 into the cisterna magna. *Mol. Ther. Methods Clin. Dev.* *1*, 14051.
- Hinderer, C., Katz, N., Dyer, C., Goode, T., Johansson, J., Bell, P., Richman, L., Buza, E., and Wilson, J.M. (2020). Translational feasibility of lumbar puncture for intrathecal AAV administration. *Mol. Ther. Methods Clin. Dev.* *17*, 969–974.
- Hinderer, C., Bell, P., Katz, N., Vite, C.H., Louboutin, J.P., Bote, E., Yu, H., Zhu, Y., Casal, M.L., Bagel, J., et al. (2018). Evaluation of intrathecal routes of administration for adeno-associated viral vectors in large animals. *Hum. Gene Ther.* *29*, 15–24.
- Sopelsa, A.M., Severini, M.H., Da Silva, C.M., Tobo, P.R., Giugliani, R., and Coelho, J.C. (2000). Characterization of beta-galactosidase in leukocytes and fibroblasts of GM1 gangliosidosis heterozygotes compared to normal subjects. *Clin. Biochem.* *33*, 125–129.
- Sandhoff, K., and Harzer, K. (2013). Gangliosides and gangliosidoses: principles of molecular and metabolic pathogenesis. *J. Neurosci.* *33*, 10195–10208.
- Leinekugel, P., Michel, S., Conzelmann, E., and Sandhoff, K. (1992). Quantitative correlation between the residual activity of beta-hexosaminidase A and arylsulphatase A and the severity of the resulting lysosomal storage disease. *Hum. Genet.* *88*, 513–523.

23. Conzelmann, E., and Sandhoff, K. (1983). Partial enzyme deficiencies: residual activities and the development of neurological disorders. *Dev. Neurosci.* 6, 58–71.
24. Fratantoni, J.C., Hall, C.W., and Neufeld, E.F. (1968). Hurler and Hunter syndromes: mutual correction of the defect in cultured fibroblasts. *Science* 162, 570–572.
25. Hordeaux, J., Hinderer, C., Goode, T., Buza, E.L., Bell, P., Calcedo, R., Richman, L.K., and Wilson, J.M. (2018). Toxicology study of intra-cisterna magna adeno-associated virus 9 expressing iduronate-2-sulfatase in rhesus macaques. *Mol. Ther. Methods Clin. Dev.* 10, 68–78.
26. Hordeaux, J., Hinderer, C., Goode, T., Katz, N., Buza, E.L., Bell, P., Calcedo, R., Richman, L.K., and Wilson, J.M. (2018). Toxicology study of intra-cisterna magna adeno-associated virus 9 expressing human alpha-L-iduronidase in rhesus macaques. *Mol. Ther. Methods Clin. Dev.* 10, 79–88.
27. Meseck, E.K., Guibinga, G., Wang, S., McElroy, C., Hudry, E., and Mansfield, K. (2021). Intrathecal Sc-AAV9-CB-GFP: Systemic Distribution Predominates Following Single-Dose Administration in Cynomolgus Macaques (Cold Spring Harbor Laboratory).
28. Pardridge, W.M. (2015). Targeted delivery of protein and gene medicines through the blood-brain barrier. *Clin. Pharmacol. Ther.* 97, 347–361.
29. Hordeaux, J., Buza, E.L., Dyer, C., Goode, T., Mitchell, T.W., Richman, L., Denton, N., Hinderer, C., Katz, N., Schmid, R., et al. (2020). Adeno-associated virus-induced dorsal root ganglion pathology. *Hum. Gene Ther.* 31, 808–818.
30. Hordeaux, J., Hinderer, C., Buza, E.L., Louboutin, J.P., Jahan, T., Bell, P., Chichester, J.A., Tarantal, A.F., and Wilson, J.M. (2019). Safe and sustained expression of human iduronidase after intrathecal administration of adeno-associated virus serotype 9 in infant rhesus monkeys. *Hum. Gene Ther.* 30, 957–966.
31. Buss, N., Lanigan, L., Zeller, J., Cissell, D., Metea, M., Adams, E., Higgins, M., Kim, K.H., Budzynski, E., Yang, L., et al. (2022). Characterization of AAV-mediated dorsal root ganglionopathy. *Mol. Ther. Methods Clin. Dev.* 24, 342–354.
32. Hinderer, C., Bell, P., Gurda, B.L., Wang, Q., Louboutin, J.P., Zhu, Y., Bagel, J., O'Donnell, P., Sikora, T., Ruane, T., et al. (2014). Intrathecal gene therapy corrects CNS pathology in a feline model of mucopolysaccharidosis I. *Mol. Ther.* 22, 2018–2027.
33. Haurigot, V., Marcó, S., Ribera, A., Garcia, M., Ruzo, A., Villacampa, P., Ayuso, E., Añor, S., Andaluz, A., Pineda, M., et al. (2013). Whole body correction of mucopolysaccharidosis IIIA by intracerebrospinal fluid gene therapy. *J. Clin. Invest.* 123, 3254–3271.
34. Marcó, S., Haurigot, V., Jaén, M.L., Ribera, A., Sánchez, V., Molas, M., Garcia, M., León, X., Roca, C., Sánchez, X., et al. (2021). Seven-year follow-up of durability and safety of AAV CNS gene therapy for a lysosomal storage disorder in a large animal. *Mol. Ther. Methods Clin. Dev.* 23, 370–389.
35. Perez, B.A., Shutterly, A., Chan, Y.K., Byrne, B.J., and Corti, M. (2020). Management of neuroinflammatory responses to AAV-mediated gene Therapies for neurodegenerative diseases. *Brain Sci.* 10, E119.
36. Broekman, M.L.D., Comer, L.A., Hyman, B.T., and Sena-Esteves, M. (2006). Adeno-associated virus vectors serotyped with AAV8 capsid are more efficient than AAV-1 or -2 serotypes for widespread gene delivery to the neonatal mouse brain. *Neuroscience* 138, 501–510.
37. Rockwell, H.E., McCurdy, V.J., Eaton, S.C., Wilson, D.U., Johnson, A.K., Randle, A.N., Bradbury, A.M., Gray-Edwards, H.L., Baker, H.J., Hudson, J.A., et al. (2015). AAV-mediated gene delivery in a feline model of Sandhoff disease corrects lysosomal storage in the central nervous system. *ASN Neuro.* 7, 1759091415569908.
38. Hauser, E.C., Kasperzyk, J.L., d'Azzo, A., and Seyfried, T.N. (2004). Inheritance of lysosomal acid beta-galactosidase activity and gangliosides in crosses of DBA/2J and knockout mice. *Biochem. Genet.* 42, 241–257.